



Published in final edited form as:

*J Am Chem Soc.* 2012 September 5; 134(35): 14298–14301. doi:10.1021/ja305579h.

## Metavanadate at the active site of the phosphatase VHZ

Vyacheslav I. Kuznetsov<sup>a</sup>, Anastassia N. Alexandrova<sup>b</sup>, and Alvan C. Hengge<sup>a</sup>

<sup>a</sup>Department of Chemistry and Biochemistry, Utah State University, Logan, UT 84322-0300

<sup>b</sup>Department of Chemistry and Biochemistry, University of California, Los Angeles, CA 90095-1569

### Abstract

Vanadate is a potent modulator of a number of biological processes and has been shown by crystal structures and NMR to interact with numerous enzymes. Although these effects often occur under conditions where oligomeric forms dominate, crystal structures and NMR data suggest the inhibitory form is usually monomeric orthovanadate, a particularly good inhibitor of phosphatases due to its ability to form stable trigonal-bipyramidal complexes. We performed a computational analysis of a 1.14 Å structure of the phosphatase VHZ in complex with an unusual metavanadate species, and compared it with two classical trigonal-bipyramidal vanadate-phosphatase complexes. The results support extensive delocalized bonding to the apical ligands in the classical structures. In contrast, in the VHZ metavanadate complex the central, planar VO<sub>3</sub> moiety has only one apical ligand, the nucleophilic cysteine-95, and a gap in electron density between vanadium and sulfur. A computational analysis shows the V-S interaction is primarily ionic. A mechanism is proposed to explain the formation of metavanadate in the active site from a dimeric vanadate species that previous crystallographic evidence shows can bind to the active sites of phosphatases related to VHZ. Together, the results show that the interaction of vanadate with biological systems is not solely reliant upon the prior formation of a particular inhibitory form in solution. The catalytic properties of an enzyme may act upon the oligomeric forms primarily present in solution to generate species such as the metavanadate ion observed in the VHZ structure.

Because of vanadate's ability to modulate a number of biological processes there is considerable interest in the origin of the interactions of this simple inorganic species with proteins.<sup>1–8</sup> Over 173 structures in the Protein Data Bank (PDB) display the interactions of different vanadate forms with a broad number of enzymes from multiple organisms.<sup>9–13</sup> Vanadate is a potent inhibitor of many phosphatases, enzymes with key roles in biological signaling throughout the living world. In particular, the insulin mimetic effect of vanadate is associated with its inhibition of protein tyrosine phosphatases (PTPs).<sup>14,15</sup> Compared to orthophosphate ion (PO<sub>4</sub><sup>3-</sup>), orthovanadate ion (VO<sub>4</sub><sup>3-</sup>) is a more potent inhibitor of phosphatases with a K<sub>i</sub> that is often several orders of magnitude lower. This difference is attributed to the ability of vanadate to form a trigonal bi-pyramidal complex at the active site, resembling the transition state for phosphoryl transfer.<sup>13,16–20</sup> Experimental data with PTPs indicate that both formation and hydrolysis of the phosphoenzyme intermediate proceed via a loose transition state with low bond orders to the nucleophile and the departing leaving group,<sup>21–24</sup> whereas crystal structures of trigonal bi-pyramidal vanadate complexes in enzymes are commonly modeled with full bonds to the apical ligands. Previous experimental and computational results suggest that such complexes resemble the transition

Correspondence to: Anastassia N. Alexandrova; Alvan C. Hengge.

Supporting Information. The absolute energies (in Hartrees) and the atomic coordinates of the computationally analyzed structures. This material is available free of charge via the Internet at <http://pubs.acs.org>.

state only in overall geometry and charge, whereas the bond orders between vanadium and the apical ligands are higher than those of the corresponding bonds in the transition state.<sup>25,26</sup>

An understanding of the inhibitory effect of vanadate on phosphatases, and of its biological effects, is complicated by the tendency of vanadate to oligomerize in solution.<sup>27</sup> These effects are frequently observed under conditions where vanadate is primarily oligomerized and the monomer is a minor form.<sup>3,27</sup> Interestingly, even though crystallization conditions often require vanadate concentrations that would primarily result in oligomeric species, crystal structures almost exclusively show monomeric vanadate at the active site. This has been attributed to the facile interconvertability of different vanadate species in solution and the ability of the active site of phosphatases to selectively stabilize the monomeric form.<sup>28</sup> Here, we report results indicating that the classical trigonal bi-pyramidal vanadate species is not the only form capable of binding to PTPs, and that other forms contribute to the inhibition of PTPs and potentially to other biological effects of vanadate.

VHZ<sup>a</sup> is a recently described member of the PTP family of phosphatases.<sup>29</sup> A recently obtained high-resolution structure of VHZ in complex with vanadate revealed what appeared to be an unusual “metavanadate” in the active site (Figure 1; PDB ID 4ERC). The VO<sub>3</sub> moiety is coordinated to the sulfur atom of cysteine 95 as one apical ligand, with a 2.4 Å V-S distance. The opposite apical position is occupied by a nitrogen atom of the arginine 60 (R<sup>S</sup>60) side chain trapped in the active site from a symmetry-related VHZ molecule in the crystal (Figure 2A). The V-N distance of 3.2 Å argues against a significant bonding interaction, nor would a significant interaction be expected with the positively charged guanidinium group. Although the V-S distance is typical of those commonly observed in trigonal bi-pyramidal vanadate-PTP complexes,<sup>17</sup> a distinct electron density gap between the atoms is evident in the high resolution unbiased composite omit map (Figure 1). Furthermore, the VO<sub>3</sub> moiety is nearly planar, while a tetrahedral geometry would be expected from a covalent V-S bond and the absence of an apical V-N bond.<sup>20,30</sup> These observations suggest that the VO<sub>3</sub> moiety is better described as an electrostatically stabilized metavanadate (VO<sub>3</sub><sup>-</sup>) rather than a covalent thiovanadate adduct. A computational analysis of this structure was carried out to analyze the unusual bonding in this complex, compared with more typical, previously reported vanadate-PTP structures (Figure 2). The two more conventional structures chosen for comparison were the complex of PTP1B with a vanadate ester of the peptide DADEYL (Figure 2B, PDB ID 3I7Z), and PTP1B with orthovanadate (Figure 2C, PDB ID 3I80). Both of the latter structures are typical of the trigonal bi-pyramidal vanadate-PTP complexes well represented in the literature. The nature of the chemical bonding between the VO<sub>3</sub> ion and the protein was assessed using quantum mechanical calculations. For this purpose portions of the proteins shown in Figure 2 were extracted directly from the crystal structures.

Truncation was done to include all residues interacting with vanadate; all residues with hydrogen bonds or pi-stacking to residues that interact with vanadate; and all groups that are polar or charged, and located in proximity to the vanadate ion even if they do not directly interact. Hydrogen atoms were added to satisfy all dangling valencies using the *Chimera* program.<sup>31</sup> The standard protonation states of amino acids were assumed (deprotonated Asp, Glu, protonated Lys and Arg), except for the Tyr coordinating vanadium in Figure 2B, which was deprotonated. The nucleophilic cysteine was assumed to be deprotonated; this residue has a pK<sub>a</sub> in the range of 5.5 to 6 in this enzyme family.<sup>32</sup> The truncated complexes effectively contained the first and the second coordination spheres of the vanadate ion, and consisted of 140–170 atoms (including hydrogens), depending on the complex. The spin

<sup>a</sup>The name VHZ denotes VH1-like member Z, one of the group of small *Vaccinia* virus VH1-related dual specific phosphatases.

states of the complexes were zero, assuming the empty d-shell in vanadium. The Natural Bond Orbital (NBO) analysis,<sup>33–36</sup> at the B3LYP<sup>37–39</sup>/6-31G\*<sup>40,41</sup> level of theory, was used to elucidate the chemical bonds present in the complexes. This level of approximation, including the fairly modest size of the basis set, were considered adequate for the problem at hand, because NBO results in general are quite insensitive to the basis set used, and because only the qualitative assessment was required to differentiate the state of V in the complexes. Calculations were performed using the *Gaussian 09* suite of programs<sup>42</sup>.

Table 1 contains the key electronic structure parameters characterizing the vanadium atom and its bonding environment in the three complexes. There is an apparent difference between the bonding exhibited by VHZ complex containing VO<sub>3</sub> (Figure 2A) and the other two complexes. As expected from its distance of 3.2 Å, there is no significant interaction between the V and the apical N of R<sup>s</sup>60. The partially populated lone pair (LP) on N of the distant apical Arg (1.66 |e|) donates electron density to the guanidinium group, participating in  $\pi$ -resonance, and is only weakly coordinated to V through Van der Waals interactions. One of the O atoms of the VO<sub>3</sub> ion exhibits a pi bond with V, representing one of the resonance structures (the lowest energy one) possible in this  $\pi$ -delocalized VO<sub>3</sub> ion. There is a clear 2 center – 2 electron (2c-2|e|) bond between V and S<sub>Cys</sub><sup>95</sup>. This bond is primarily ionic, with 79% of electron density residing on S and 21% on V. This is consistent with the electron density gap observed in the unbiased composite omit map between the C95 sulfur and V, which is indicative of ionic rather than covalent ligand stabilization. The bonding within the vanadate moiety and its interaction with VHZ differ in several ways from the more conventional PTP1B complexes. In contrast to the VHZ-VO<sub>3</sub> complex 2A, in the PTP1B complexes 2B and 2C there is no  $\pi$ -bonding within the central VO<sub>3</sub> part of the ion. This is reflected in different averaged V-O bond lengths in the x-ray structures, which are 1.70 Å for 2A, 1.89 Å for 2B, and 1.91 Å for 2C. One lone pair on S<sub>Cys</sub><sup>215</sup> (LP3) and one on O<sub>Tyr</sub> (LP3) are populated only by ca. 1.7 |e|, within the NBO localized picture. The low-populated lone pair on S (LP3) partially donates electron density to the d-atomic orbitals (AOs) of vanadium. The low-populated lone pair on O of Tyr (LP3) primarily donates electrons into 3-resonance within the Tyr phenyl ring. However, both LP2 and LP3 on O<sub>Tyr</sub> also donate to the d-AOs on vanadium.

To summarize, in complexes 2B and 2C neither the V-S<sub>Cys</sub>, nor the V-O<sub>Tyr</sub> apical interactions are classic 2c-2|e| bonds. Bonding between vanadium and these apical ligands is significant and highly delocalized between S<sub>Cys</sub>, V, and O<sub>Tyr</sub>. The equatorial V-O interactions are single bonds. In contrast, the complex 2A can be described as a  $\pi$ -delocalized VO<sub>3</sub> ion with only one apical interaction, an ionic bond between V and S<sub>Cys</sub>. PTP-VO<sub>4</sub> complex 2C.

The complex solution chemistry of vanadate must be considered together with the chemical properties of the enzymes it can associate with. Monomeric vanadate dominates at low concentrations, with dimeric forms becoming significant at concentrations above 0.2 mM, followed by higher oligomers.<sup>28</sup> Interconversion is rapid, and it is logical that the various forms of vanadate should be similarly labile in an enzymatic active site. There is no reason, *a priori*, that an inhibiting form of vanadate must pre-form in solution before binding to the enzyme. While numerous oligomeric forms of vanadate have been documented, metavanadate has not been reported in solution, and presumably was generated by the enzyme from some other vanadate species present in solution, and subsequently stabilized by the active site environment. We propose a simple mechanism that can explain the formation of this species from divanadate, and possibly polyvanadate, forms that are well known to exist, and usually dominate, in solution. In light of the highly conserved nature of the active sites of PTPs, this mechanism would apply to this family as whole, and potentially to any similar enzyme with a general acid. This proposal (Figure 3) incorporates the general

acid conserved in PTPs, and also explains why the first report of a divanadate species at the active site of a PTP was found in a YopH W354F mutant in which the flexible loop that bears the general acid is locked in a catalytically unproductive position.<sup>43</sup> The crystal structure of this divanadate complex showed that dimeric, and possibly higher oligomeric species, are capable of binding to PTPs (Figure 3D). We believe it is no coincidence that this complex was identified in a mutant in which general acid catalysis is disabled. Presumably, this or other dimeric forms bind to the native enzyme, but are rapidly hydrolyzed to the monomer and not observed crystallographically.

According to the proposed mechanism, divanadate (Figure 3D) binds in the active site and the general acid protonates one of its bridge oxygens, triggering decomposition and formation of “metavanadate”, stabilized by the P-loop and electrostatic interaction with the nucleophilic thiolate. The resulting complex (Figure 3E) is the species trapped in the VHZ-VO<sub>3</sub> crystal structure. The classically observed trigonal bi-pyramidal orthovanadate species can result from a process analogous to the second step of the PTP-catalyzed reaction, in which a nucleophilic water attacks with positioning assistance of Q-loop residues, assuming the other apical position. Such a process would explain the high affinity and selectivity in crystal structures of PTPs for monomeric orthovanadate under conditions where oligomeric polyvanadates dominate in solution. Recent work<sup>44</sup> shows that vanadate speciation is sensitive to surfaces such as micelles, consistent with the idea that an enzyme active site could preferentially stabilize a species such as the dimer in 3D, or metavanadate.

We note that the reversible interconversion between F and G in Figure 3 provides an alternative pathway for enzyme-catalyzed metavanadate formation without invoking binding of a dimeric form. However, the VHZ crystals were grown in the presence of 10 mM vanadate, far above the 0.2 mM level at which dimeric and higher forms begin to dominate. Potent vanadate inhibition of many phosphatases is reported across wide ranges of pH and vanadate concentrations, supporting the notion that multiple forms are capable of binding, and that the interconvertibility in the active site is similar to that in solution. If anything, the active site of an enzyme optimized to catalyze hydrolysis should facilitate such processes.

The metavanadate species observed here is not an anomalous structure only relevant to VHZ, or potentially other PTPs. A geometrically similar VO<sub>3</sub> species has been previously observed in a crystal structure of phosphoglucomutase,<sup>45</sup> an enzyme that has no similarity to PTPs. That structure also reveals a planar VO<sub>3</sub> moiety with a single apical ligand (an aspartate carboxyl group) and a similar gap in the 2Fo-Fc electron density obtained from the Electron Density Server (EDS) observed at 1.0  $\sigma$ .

In summary, this work shows that the interaction of vanadate with the active sites of PTPs in solution is more versatile than the simple trigonal bi-pyramidal model that dominates the RCSB. The inhibitory effect of vanadate can involve dimeric, and potentially higher oligomers, an important factor since such species often dominate in solution. The ability of the active site environment to electrostatically stabilize a metavanadate ion adds another facet to the interaction of vanadate with such enzymes. In the VHZ-VO<sub>3</sub> complex there is only a single significant apical interaction, which is primarily ionic.

This complex is a good analogue of the loose metaphosphate-like transition state concluded from experimental studies. The average V-O<sub>eq</sub> bond distance in the VHZ-VO<sub>3</sub> structure is shorter compared to the commonly observed trigonal bi-pyramidal vanadate complexes, but in a good agreement with experimental values determined with Raman difference spectroscopy of vanadate at the active site of the related enzyme YopH.<sup>25</sup> Hence, it is conceivable that such VO<sub>3</sub> species may form more commonly than suspected in PTP-vanadate solutions, and the dominance among crystal structures of the trigonal bi-pyramidal

structures (like 3E and 3F) arise from species that subsequently form and are more amenable to trapping. The rich speciation of vanadate in solution clearly extends to its ability to also adopt multiple species at enzymatic active sites.

## Supplementary Material

Refer to Web version on PubMed Central for supplementary material.

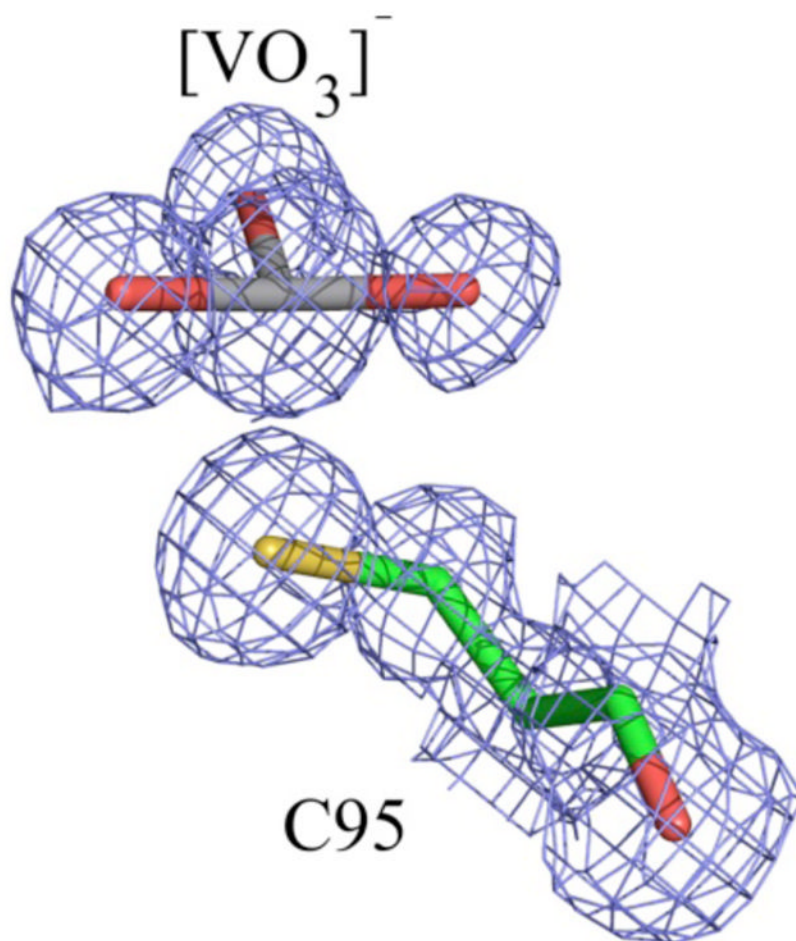
## Acknowledgments

This work was supported by NIH grant GM 47297 (ACH), and a DARPA Young Faculty Award N66001-11-1-4138 (ANA).

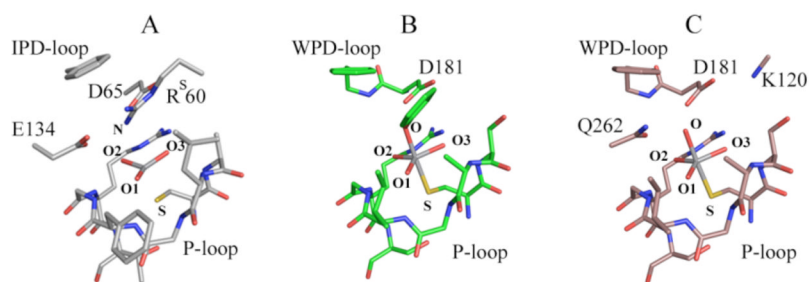
## References

1. Bishayee A, Waghay A, Patel MA, Chatterjee M. *Cancer Lett.* 2010; 294:1. [PubMed: 20206439]
2. Cam MC, Brownsey RW, McNeill JH. *Can J Physiol Pharmacol.* 2000; 78:829. [PubMed: 11077984]
3. Crans DC, Smee JJ, Gaidamauskas E, Yang L. *Chem Rev.* 2004; 104:849. [PubMed: 14871144]
4. Evangelou AM. *Crit Rev Oncol Hematol.* 2002; 42:249. [PubMed: 12050018]
5. Heyliger CE, Tahiliani AG, McNeill JH. *Science.* 1985; 227:1474. [PubMed: 3156405]
6. Rubinson KA. *Proc R Soc Lond B Biol Sci.* 1981; 212:65. [PubMed: 6115390]
7. Tsiani E, Bogdanovic E, Sorisky A, Nagy L, Fantus IG. *Diabetes.* 1998; 47:1676. [PubMed: 9792535]
8. Tsiani E, Fantusa IG. *Trends in Endocrinology and Metabolism.* 1997; 8:51. [PubMed: 18406786]
9. Crans DC, Sudhakar K, Zamborelli TJ. *Biochemistry.* 1992; 31:6812. [PubMed: 1637817]
10. Crans DC, Willging EM, Butler SR. *JACS.* 1989; 112:427.
11. Messmore JM, Raines RT. *Journal of the American Chemical Society.* 2000; 122:9911. [PubMed: 21423825]
12. Messmore JM, Raines RT. *Archives of biochemistry and biophysics.* 2000; 381:25. [PubMed: 11019816]
13. Stankiewicz PJ, Gresser MJ. *Biochemistry.* 1988; 27:206. [PubMed: 3280015]
14. Shechter Y. *Diabetes.* 1990; 39:1. [PubMed: 2210051]
15. Bhattacharyya S, Tracey AS. *J Inorg Biochem.* 2001; 85:9. [PubMed: 11377690]
16. Zhang M, Zhou M, Van Etten RL, Stauffacher CV. *Biochemistry.* 1997; 36:15. [PubMed: 8993313]
17. Brandao TA, Hengge AC, Johnson SJ. *J Biol Chem.* 2010; 285:15874. [PubMed: 20236928]
18. Davies DR, Hol WG. *FEBS Lett.* 2004; 577:315. [PubMed: 15556602]
19. Stankiewicz PJ, Tracey AS, Crans DC. *Met Ions Biol Syst.* 1995; 31:287. [PubMed: 8564811]
20. Denu JM, Lohse DL, Vijayalakshmi J, Saper MA, Dixon JE. *PNAS.* 1996; 93:2493. [PubMed: 8637902]
21. Lassila JK, Zalatan JG, Herschlag D. *Annu Rev Biochem.* 2011; 80:669. [PubMed: 21513457]
22. Hengge AC. *Advances in Physical Organic Chemistry.* 2005; 40:49.
23. Hengge AC, Zhao Y, Wu L, Zhang ZY. *Biochemistry.* 1997; 36:7928. [PubMed: 9201938]
24. Hengge AC, Sowa GA, Wu L, Zhang ZY. *Biochemistry.* 1995; 34:13982. [PubMed: 7577995]
25. Krauss M, Basch H. *J Am Chem Soc.* 1992; 114:3630.
26. Deng HCR, Huang Z, Zhang ZY. *Biochemistry.* 2002; 41:5865. [PubMed: 11980490]
27. Crans DC, Bunch RL, Theisen LA. *J Am Chem Soc.* 1989; 111:7597.
28. Crans DC, Rithner CD, Theisen LA. *J Am Chem Soc.* 1990; 112:2901.
29. Alonso A, Burkhalter S, Sasin J, Tautz L, Bogetz J, Huynh H, Bremer MC, Holsinger LJ, Godzik A, Mustelin T. *J Biol Chem.* 2004; 279:35768. [PubMed: 15201283]
30. Pannifer AD, Flint AJ, Tonks NK, Barford D. *J Biol Chem.* 1998; 273:10454. [PubMed: 9553104]

31. Pettersen EF, Goddard TD, Huang CC, Couch GS, Greenblatt DM, Meng EC, Ferrin TE. *J Comput Chem.* 2004; 25:1605. [PubMed: 15264254]
32. Denu JM, Dixon JE. *Proc Natl Acad Sci U S A.* 1995; 92:5910. [PubMed: 7597052]
33. Carpenter JE, Weinhold F. *J Mol Struct (THEOCHEM).* 1988; 41–62:169.
34. Foster JP, Weinhold F. *J Am Chem Soc.* 1980; 102:7211.
35. Reed AE, Weinhold F. *J Chem Phys.* 1983; 78:4066.
36. Reed AE, Curtiss LA, Weinhold F. *Chem Rev.* 1988; 88:899.
37. Parr, RG.; Yang, W. Oxford Univ. Press; Oxford: 1989.
38. Becke AD. *J Chem Phys.* 1993; 98:5648.
39. Perdew JP, Chevary JA, Vosko SH, Jackson KA, Pederson MR, Singh DJ, Fiolhais C. *Phys Rev B.* 1992; 46:6671.
40. Clark TCJ, Spitznagel CW, Schleyer PvR. *J Comput Chem.* 1983; 4:294.
41. Frisch MJPA, Binkley JS. *J Chem Phys.* 1984; 80:3265.
42. RA; Frisch, MJ.; Trucks, GW.; Schlegel, HB.; Scuseria, GE.; Robb, MA.; Cheeseman, JR.; Scalmani, G.; Barone, V.; Mennucci, B.; Petersson, GA.; Nakatsuji, H.; Caricato, M.; Li, X.; Hratchian, HP.; Izmaylov, AF.; Bloino, J.; Zheng, G.; Sonnenberg, JL.; Hada, M.; Ehara, M.; Toyota, K.; Fukuda, R.; Hasegawa, J.; Ishida, M.; Nakajima, T.; Honda, Y.; Kitao, O.; Nakai, H.; Vreven, T.; Montgomery, JA., Jr; Peralta, JE.; Ogliaro, F.; Bearpark, M.; Heyd, JJ.; Brothers, E.; Kudin, KN.; Staroverov, VN.; Kobayashi, R.; Normand, J.; Raghavachari, K.; Rendell, A.; Burant, JC.; Iyengar, SS.; Tomasi, J.; Cossi, M.; Rega, N.; Millam, NJ.; Klene, M.; Knox, JE.; Cross, JB.; Bakken, V.; Adamo, C.; Jaramillo, J.; Gomperts, R.; Stratmann, RE.; Yazyev, O.; Austin, AJ.; Cammi, R.; Pomelli, C.; Ochterski, JW.; Martin, RL.; Morokuma, K.; Zakrzewski, VG.; Voth, GA.; Salvador, P.; Dannenberg, JJ.; Dapprich, S.; Daniels, AD.; Farkas, Ö.; Foresman, JB.; Ortiz, JV.; Cioslowski, J.; Fox, DJ. *Gaussian 09. Gaussian, I; Wallingford, CT., editors.* 2009.
43. Brandao TA, Robinson H, Johnson SJ, Hengge AC. *J Am Chem Soc.* 2009; 131:778. [PubMed: 19140798]
44. Crans DC, Baruah B, Ross A, Levinger NE. *Coordin Chem Rev.* 2009; 253:2178.
45. Lu Z, Dunaway-Mariano D, Allen KN. *Proc Natl Acad Sci U S A.* 2008; 105:5687. [PubMed: 18398008]

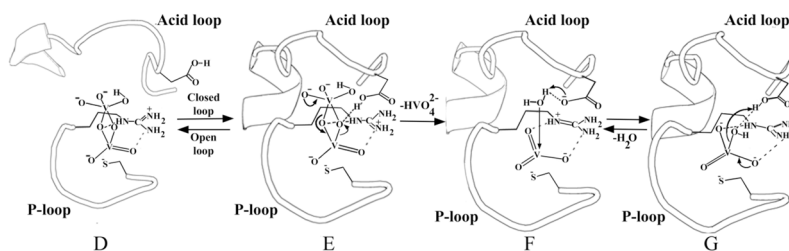


**Figure 1.** The electron density at the VHZ active site suggests a non-covalently bound VO<sub>3</sub><sup>-</sup> ion. Shown is an unbiased composite omit map contoured at 1.5  $\sigma$  in the refined model.



**Figure 2.** The regions of the three vanadate complexes used in quantum mechanical calculations. (A) VHZ-VO<sub>3</sub> (PDB 4ERC) (B) PTP1B-Tyr-VO<sub>4</sub> (PDB 3I7Z), (C) PTP1B-VO<sub>4</sub> (PDB 3I80). Hydrogens have been omitted from the picture for the sake of clarity. In the VHZ complex, the R<sup>S</sup>60 residue in the active site comes from a symmetry-related VHZ molecule. DADEYL peptide was omitted with exception of Y side chain.



**FIGURE 3.**

A proposed mechanism that explains the formation of a metavanadate species in the active site of VHZ. The vanadium species D, F and G have been observed in crystal structures. Protonation states of the vanadium species are not known from the crystal structures, but are depicted in states consistent with the pH at which crystals were grown. D) PDB ID 3F9B - divanadate bound in the active site of the YopH mutant W354F with catalytic WPD (acid)-loop locked in a half-open conformation; E) transient complex (not observed in the crystal form) showing the acid-loop closure which triggers the catalytic transformation of divanadate into metavanadate; VHZ has no mobile loop but its general acid occupies an analogous position. F) PDB ID 4ERC- metavanadate trapped in the active site of VHZ; G) PDB ID 3I80 - orthovanadate in the active site of PTP1B.

**Table 1**

Electronic structure parameters characterizing the vanadium atom and its bonding in complexes 2A–C, calculated with NBO at B3LYP/6-31G\*: Charges on atoms (Q), electronic populations of 2 center-2 electron (2c-2|e|)  $\sigma$  and bonds, and  $\pi$  electronic populations of lone pairs (LP). Atoms are labeled according to Figure 2.

	VO <sub>3</sub> (2A)	VO <sub>4</sub> (2B)	VO <sub>4</sub> (2C)
Q(V)	+1.09	+1.34	+1.33
Q(S <sub>Cys</sub> )	-0.31	-0.42	-0.42
Q(N/O <sub>apical</sub> )	-0.79 <sup>a</sup>	-0.68	-0.90
2c-2 e  bonds:			
V-O1	1.99  e  - $\sigma$	1.99  e	1.98  e
	1.96  e  - $\pi$	<b>none</b>	<b>none</b>
V-O2	1.98  e	1.99  e	1.99  e
V-O3	1.98  e	1.99  e	1.98  e
V-S	1.95  e	<b>none</b>	<b>none</b>
Lone pairs:			
LP1(S)	1.94  e	1.94  e	1.94  e
LP2(S)	1.87  e	1.88  e	1.88  e
LP3(S)	<b>none</b> <sup>b</sup>	1.73  e	1.73  e
V-N or O <sub>apical</sub>	<b>none</b>	<b>none</b>	<b>none</b>
LP1(N or O <sub>apical</sub> )	n/a <sup>c</sup>	1.91  e	1.94  e
LP2(O <sub>apical</sub> )	n/a	1.86  e	1.83  e
LP3(N or O <sub>apical</sub> )	1.66  e	1.61  e	1.65  e

<sup>a</sup>-0.79 is the atomic charge on the R<sup>S60</sup> nitrogen atom in an apical position to vanadium; the total charge on the guanidinium group of this arginine is +0.6.

<sup>b</sup>"none" indicates that suitable orbitals are available, but not occupied.

<sup>c</sup>"n/a" indicates that the lone pair orbitals are not present.